Advances in Environmental Technology 2 (2017) 77-87

Advances in Environmental Technology

journal homepage: http://aet.irost.ir

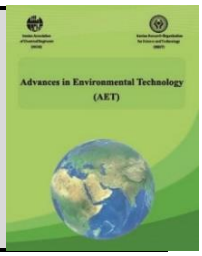

Toxic metal removal from aqueous solution by advanced carbon allotropes: A case study from the Sungun copper mine

Esmaeil Rahimi

Department of Mining Engineering, Islamic Azad University- South Tehran Branch, Tehran, Iran

ARTICLE INFO

Article history:
Received 5 February 2017
Received in revised form
21 June 2017
Accepted 24 June 2017

Keywords:
Acid mine drainage
Carbon allotropes
Graphene oxide
Multi-walled Carbon nanotubes
Sorption process
Sungun Copper mine

ABSTRACT

The sorption efficiencies of graphene oxide (GO) and functionalized multi-walled carbon nanotubes (f-MWCNTs) were investigated and elucidated to study their potential in treating acid mine drainage (AMD) containing Cu^{2+}, Mn^{2+}, Zn^{2+}, Pb^{2+}, Fe^{3+} and Cd^{2+} metal ions. Several layered GO nanosheets and f-MWCNTs were formed via the modified Hummers' method and the acid treatment of the MWCNTs, respectively. The prepared nanoadsorbents were characterized by field emission scanning electron microscopy (FE-SEM), Fourier transformed infrared (FTIR) spectroscopy, and BET surface area analysis. The batch method was utilized to evaluate the pH effect, sorption kinetics and isotherms. The results demonstrated that the sorption capacities of the MWCNTs increased greatly after oxidation and those of the GO decreased after reduction. Hence, the sorption mechanisms seemed principally assignable to the chemical interactions between the metal ions and the surface functional groups of the adsorbents. Additionally, the adsorption isotherm results clearly depicted that the adsorption of the Cu^{2+} ion onto the GO adsorbent surface was well fitted and found to be in good agreement with the Langmuir isotherm model as the obtained regression constant value (R^2) was found to be 0.9981. All results indicated that GO was a promising material for the removal of toxic metal ions from aqueous solutions in actual pollution management.

1. Introduction

The removal of toxic metal ions from aqueous sources these days turns out to be a relevant matter for researchers. Recently, the formation of acid mine drainage (AMD), highly contaminated liquid wastes, and the release of the dissolved toxic metal ions into the environment are considered more significant issues. AMD poses a serious threat to human health, animals and ecological systems due to the pyrite oxidation reaction. Drainage water contains toxic metal ion contaminants such as Cu^{2+}, Fe^{3+}, Mn^{2+}, Zn^{2+}, Cd^{2+} and Pb^{2+}. These metal ions are known to be carcinogenic and are not biodegradable; thus, they tend to accumulate in living organisms, posing a threat in the form of diseases and disorders. Therefore, increased attention and serious effort are required to remove these toxic metal ions from AMD before releasing it into the environment [1-5]. Metal ions can be removed from water resources via some traditional techniques such as sedimentation, oxidation, reduction, chemical precipitation, vacuum evaporation, ultra-filtration, ion exchange and adsorption [6,7]. Among all of the above methods, adsorption is the most promising process utilized for the removal of metal ions because it is the most efficient, particularly simple and economical. So far, different types of developed adsorbents such as carbon nanotubes, zeolite, MWCNTs, nanoparticles and nanocomposites have been tested for the rapid removal of toxic metal ions [6,7]. However, these adsorbents suffer from either low sorption capabilities or other inefficiencies. Thus, enormous efforts have been made in recent years to seek novel adsorbents and develop new techniques. The application of nanotechnology in this field is considered as one of the major solutions for solving the problem of common refining methods. Due to their

*Corresponding author. Tel: +98 2186022471
E-mail address: se_rahimi@azad.ac.ir
DOI: 10.22104/AET.2017.507

high special surface area, enhanced active sites, crystalline shape, unique network arrangement, abundant functional groups on the surface and high reactivity, nanoparticles or nanocomposites can be used to remove pollutants [12-16]. Graphene possesses intriguing characteristics such as electron mobility at room temperature and excellent mechanical, thermal and electrical properties; it has become a rapidly growing star among carbon materials. Graphene is considered as the mother element of some carbon allotropes, which is a main structure block for graphitic materials. Graphene and its derivatives have high special surface areas and many functional groups on the surface, causing the superior removal of metal ions from aqueous solutions [19-23]. Multi-walled carbon nanotubes (MWCNTs) or carbon nanotubes (CNTs) are one of the most commonly used building blocks of nanotechnology because of their unique structure, high mechanical strength, large specific surface area and favourable electronic properties. The walls of CNTs are not highly reactive; hence, functionalization of the CNTs wall is used relatively often to form many functional groups such as COOH, OH, or C=O. As reported before, CNTs have been proven to possess great potential as effective adsorbents for removing various kinds of pollutants from aqueous solution [24-26]. The application of GO nanosheets and f-MWCNTs is undoubtedly of special interest in both adsorption processes and AMD treatment. In the present work, the uptake efficiency of Cu^{2+}, Fe^{3+}, Mn^{2+}, Zn^{2+}, Cd^{2+} and Pb^{2+} ions from aqueous solutions similar to AMD from the Sungun copper mine in East Azerbaijan, Iran, using MWCNTs, f-MWCNTs, GO and RGO nanosheets were investigated and compared. The mechanism of metal ion sorption, sorption kinetic and isotherms were also discussed. Additionally, the effect of the pH of solution on both the sorption rate and efficiency was studied. Experiments to determine how well the prepared nanoadsorbents worked were carried out using AMD wastewater from the Sungun copper mine as a field sample.

2. Materials and methods

2.1. Materials and apparatus

The absorption spectrum of the fabricated GO and RGO were characterized via a UV-Vis spectrophotometer (GBC Cintra 40). The XRD patterns of the nanoadsorbents were recorded by a Philips X'pert instrument. The morphological characteristics were studied by Scanning Electron Microscopy (SEM, XL30 model). The FTIR spectra were reported in the transmission mode on an ABB BOMER MB series spectrophotometer in the range of 400-4000 cm^{-1}. The specific surface area and pore volume distributions of the adsorbents were estimated from the nitrogen adsorption-desorption isotherms (Belsorp apparatus). The metal ion concentrations in each sorption test were determined by atomic absorption during the removal experiments (Varian SpectrAA 220 spectrometer).

2.2. Adsorbent preparation

Several layered GO nanosheets were synthesized using the modified Hummers' method according to our previous paper [27]. For RGO fabrication, the GO was treated by the hydrothermal reduction method at 120 °C for 3 h [28]. The functionalization of the MWCNTs was performed in a mixture of sulfuric and nitric acid (50ml, 3:1v/v) under a reflux condition based on the previous study [29].

2.3. Sorption experiments

A batch reactor surrounded by a circulating water jacket to keep the temperature constant at about 25°C was used for the sorption experiments. The reactor was first filled with 200 ml of synthesized solution including metal ions with the desired concentration and then 0.1 g of adsorbents was fed into the reactor. The suspension was magnetically stirred for 120 min at 1000 rpm. At any time intervals, the solution was removed, centrifuged and submitted for Atomic Absorption Spectrophotometer analysis. By performing a proper material balance, the quantity of ions adsorbed at regular time intervals was determined.

3. Results and discussion

3.1. Characterization of Sorption Samples

The UV–Vis absorption spectrum of GO nanoadsorbent is displayed in Figure 1. There are two peaks at about 230 and 290–300 nm attributed to the $\pi \rightarrow \pi^*$ transitions of unoxidized C=C and $n \rightarrow \pi^*$ C=O bonds, respectively. The absorption peak of the GO at 230 nm red-shifts to a higher wavelength and the small shoulder around 290–300 nm disappeared after hydrothermal treatment [28] (Figure 1b). This is accompanied by a change in the colour of the GO solution from yellow brown to black, confirming the reduction of GO to RGO (Figure 1).

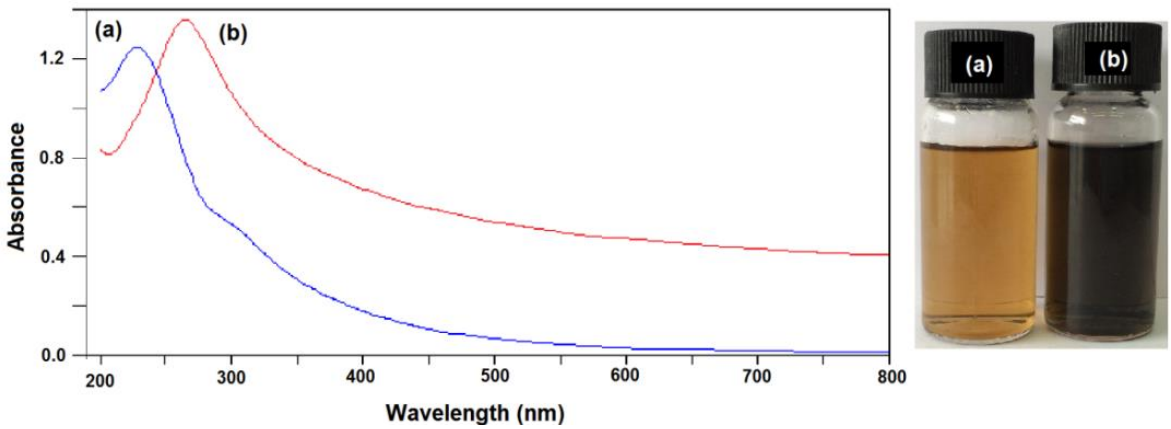

Fig. 1. (a) UV–Vis absorption spectrum and (b) the photograph of synthesized GO and RGO solutions.

3.1.1. FE-SEM analysis

SEM analysis with a field emission gun was used for investigating the surface morphological properties of the adsorbents. Figure 2a and b exhibit the surface textural properties of two developed adsorbents; it confirms their porous nature.

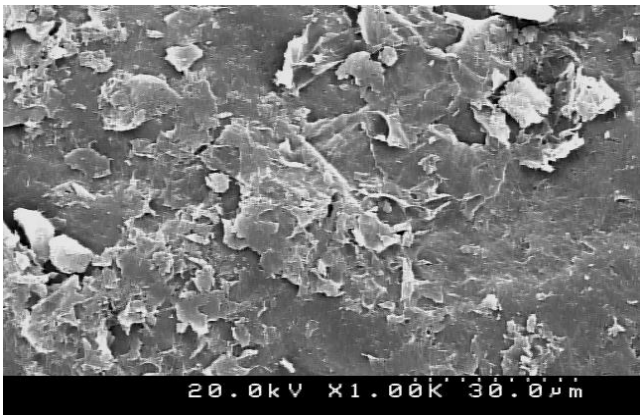

(a)

(b)

Fig. 2. SEM images of a) GO and b) f-MWCNTs.

3.1.2 FTIR spectroscopy

The FTIR spectrum of the GO nanoadsorbent is presented in Figure 3. The spectrum shown in Figure 3 clearly depicts the presence of peaks related to the main oxygen containing groups such as O-H, C=O and C-O on the surface of the GO nanoadsorbent [28]. These groups were expected to form strong surface complexes with metal ions.

The FTIR spectra of both the MWCNTs and f-MWCNTs samples are also shown in Figure 4. The absorption peak at 1600 cm^{-1} corresponded to the C=C bond of the hexagonal network in the MWCNTs. After the acid treatment, new peaks were observed. These peaks, at about 1730 cm^{-1}, 3400 cm^{-1} and 1380-1460 cm^{-1}, were ascribed to the stretching modes of C=O, O-H and the stretching modes of the C=OH bond of carboxylic acid, respectively [25].

3.1.3. BET surface area analysis

Table 1 shows the specific surface area and total pore volume information for the nanoadsorbents. A high specific surface area is generally needed to promote the adsorption capacity of toxic metal ions. As seen in Table 1, both nanoadsorbents have the highest specific surface area, showing their great potential for adsorbing various metal ions.

Table 1. Properties of the nanoadsorbents.

Adsorbents	S_{BET} (m^2/g)	Total pore volume (cm^3/g)
f-MWCNTs	196.0	0.380
GO	478.7	1.313

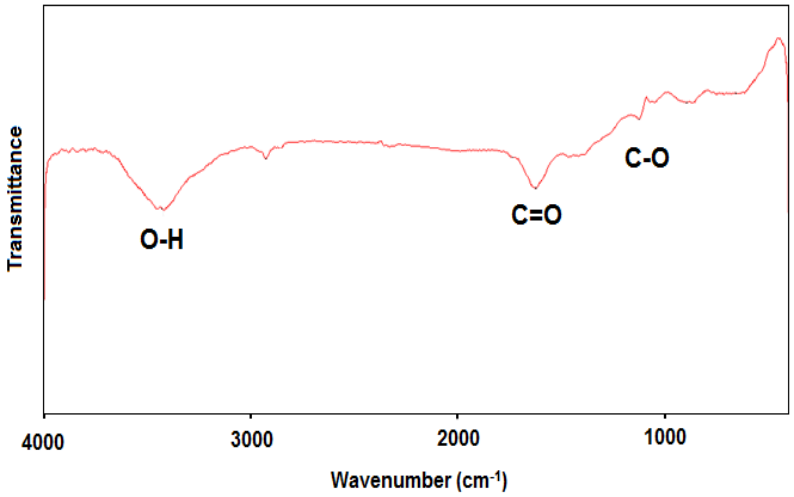

Fig. 3. FTIR spectrum of GO nanosheets.

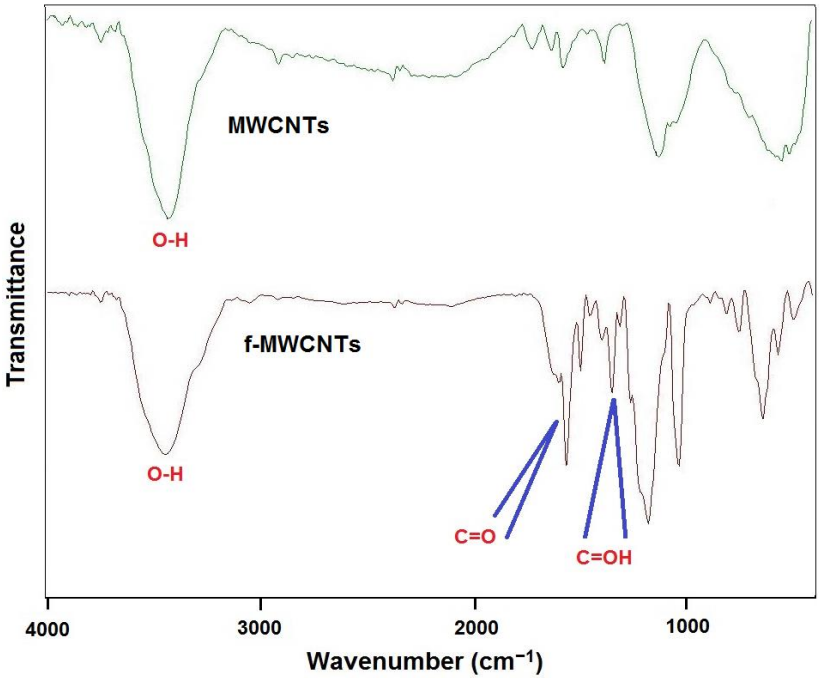

Fig. 4. FTIR spectrum of MWCNTs and f-MWCNTs.

3.2. Sorption of metal ions over adsorbents

The sorption curves of metal ions over nanoadsorbents are represented in Figure 5. As seen in Figure 5, the removal efficiency for the total metal ions over the GO nanosheets was higher than that over the f-MWCNTs adsorbent. This was thought to be due to the higher specific surface area of the synthetic GO. The sorption capacities of the metal ions by MWCNTs were low but significantly increased after oxidized by acid treatment. When the f-MWCNTs were used as a sorbent, the lower specific surface area of f-MWCNT compared to GO was approximately compensated for by its more functional groups on the surface. Oxidation treatments promoted the dispersion and also produced more functional groups such as –COOH, –OH, or –C=O on the surface sites of the f-MWCNTs. These functional groups increased negative charges on the surface of the f-MWCNTs and thus, the oxygen atoms donated a single pair of electrons to the metal ions, increasing their cation exchange.

As seen in Figure 6, the GO had a better performance on the metal ion sorption than the f-MWCNTs and RGO. There are three possible reasons to explain the greater ion sorption onto the GO. First, GO had a higher specific surface area than the MWCNTs. Second, metal ions were chemically sorbed by surrounding the metal ions with epoxides, hydroxides, carboxylic groups and carboxylate distributed on the surface of GO. As a result, the GO with many functional groups such as –O–, –OH, and –COOH can make complexes with metal ions (As observed in the FTIR spectrum). So, the adsorption activity of the GO sample was more than the RGO. Third, metal ions were eager to

accumulate along the wrinkles and edges on the surface of the GO (Based on the SEM image). Therefore, compared with the f-MWCNTs, the GO showed a higher adsorption capacity.

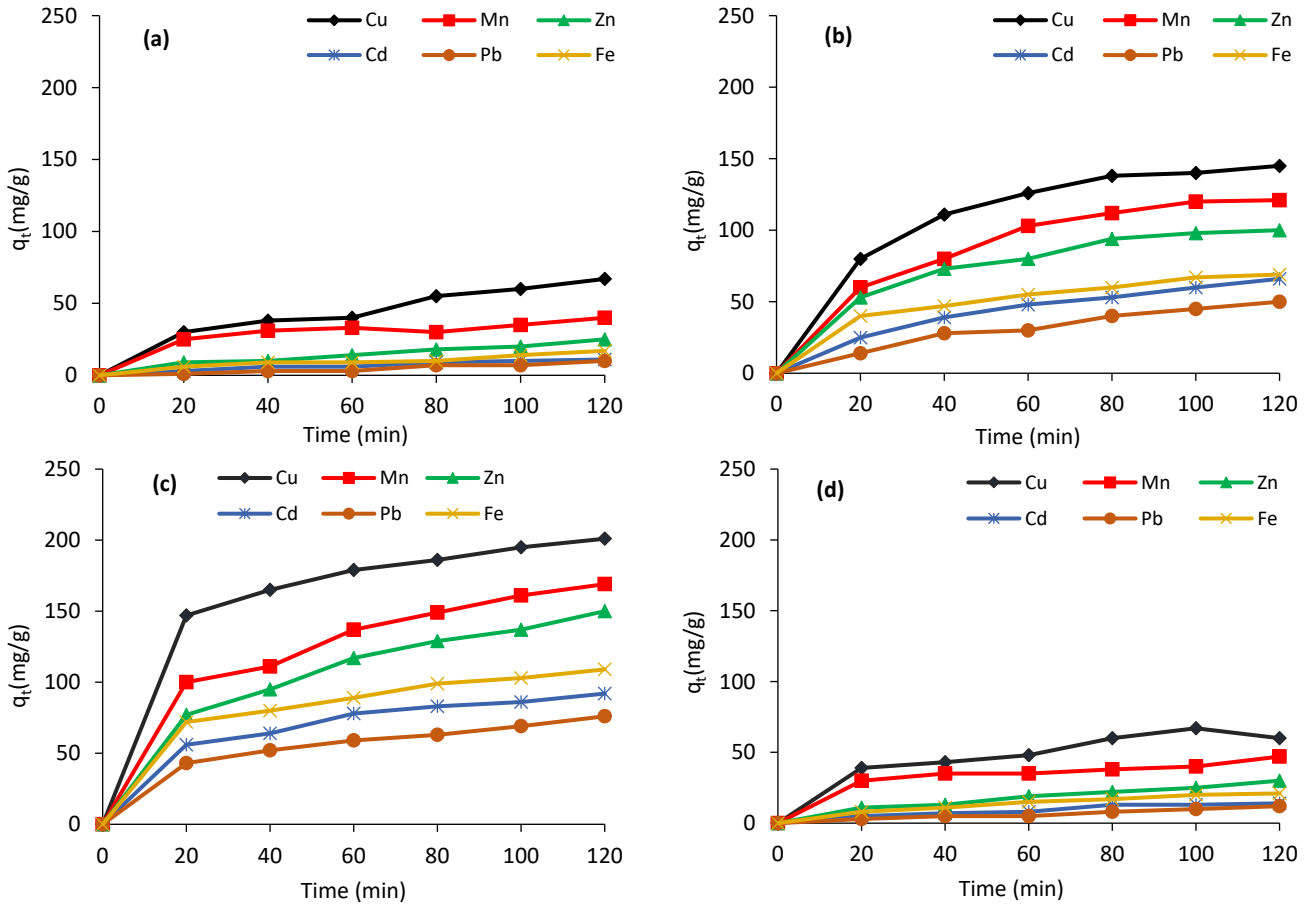

Fig. 5. Removal efficiency of metal ions from synthetic solution with (a) MWCNTs, (b) f-MWCNTs, (c) GO and (d) RGO (pH=7, Contact time=120 min, T= 25°C).

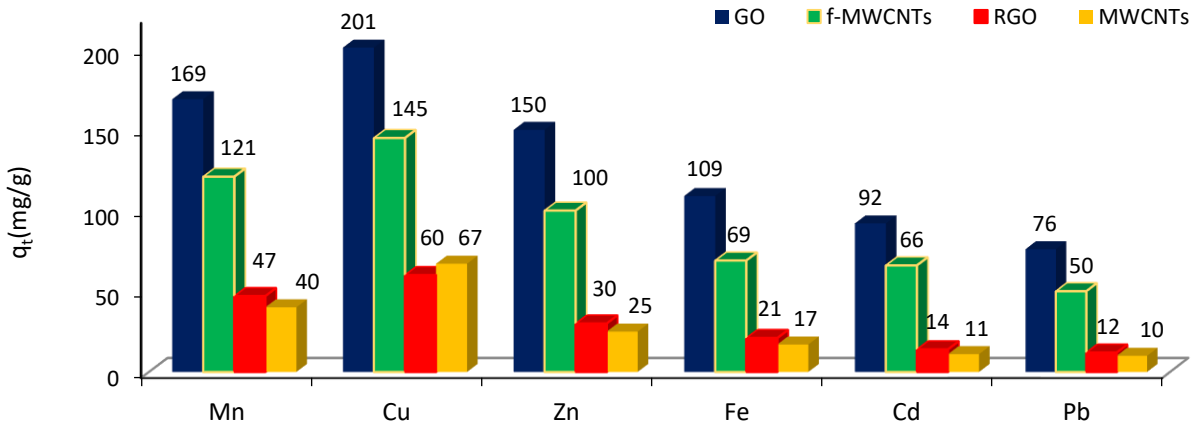

Fig. 6. The adsorption activity of MWCNTs, f-MWCNTs, GO and RGO (pH=7, Contact time=120 min, T=25°C).

For all the prepared adsorbent samples, adsorption was a heterogeneous reaction showing an initial fast adsorption followed by adsorption at a slower rate. This occurred because initially the active sites were more available and the ions interacted easily with them. This initial stage of fast adsorption corresponded to ion exchange into the pores of sorbent grains and adsorption on the surface of the sorbents. In addition, the driving force for adsorption, being the concentration difference between the bulk solution and the solid-liquid interface, was initially very high; this also

resulted in a higher adsorption rate [27]. However, after the initial period, slower adsorption may be due to the slower diffusion of metal ions into the available pores on the GO surface. Figure 7 illustrates the total removal process of metal ions with GO and f-MWCNTs.

3.3. Kinetics studies

Studying the rate of the adsorption process is one of the most important factors in designing the adsorption system. The well-known pseudo-second-order rate equations were used for studying the adsorption mechanism and kinetics for all of the metal ions and fitted well for all of them. This kinetics model was consistent with the assumption that the determining rate step could be chemical sorption consisting of valence forces formed via electronic interaction between the adsorbent and the adsorbate samples [5,30]. The pseudo-second-order chemisorption kinetics model is represented according to the Eq. 1:

$$\frac{dq_t}{dt} = k(q_e - q_t)^2 \quad (1)$$

where q_e is the amount of adsorbed per unit mass at equilibrium, q_t is the amount of metal ions adsorbed at time t (mg/g adsorbent), and k is the second order rate constant (g $mg^{-1}min^{-1}$). A linear form of the typical second-order rate equation is shown below in Eq. 2:

$$\frac{t}{q_t} = \frac{1}{h} + \frac{1}{q_e}t \quad (2)$$

And *h* can be estimated from Eq. 3.

$$h = kq_e^2 \quad (3)$$

The pseudo-second-order model constants can be calculated via plotting $\frac{t}{q_t}$ versus time (t). The kinetic sorption curves of the metal ions on the used sorbents are shown in Figure 8.

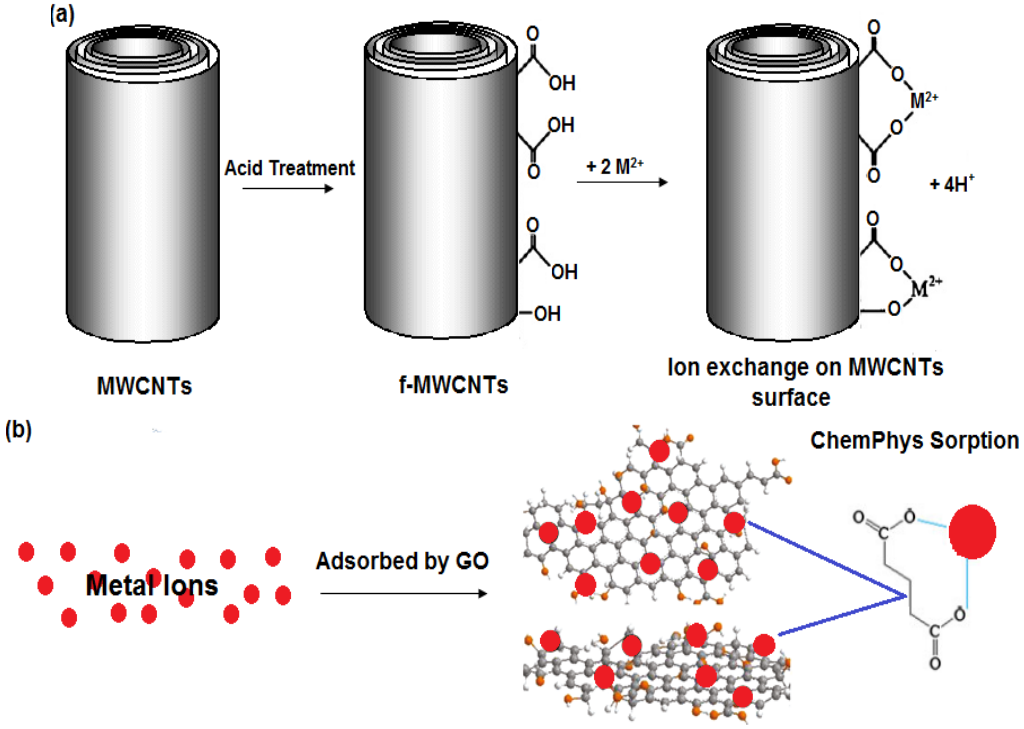

Fig.7. Total removal process of metal ions with (a) f-MWCNTs and (b) GO adsorbents.

3.4. Sorption isotherms

The aforementioned equations precisely give an account of the wide range of results presented in this work and it is believed that they can be greatly used for analysing the isotherm data. The two main isotherm models used in the analysis of the adsorption isotherms were the Langmuir and Freundlich equations. The Langmuir model was considered by the authors to be the best available for describing sorption [5,30]. The mathematical equations applied in the Langmuir adsorption isotherm are shown in Table 2. In the above equations, C_e is the metal ion concentration (mg/L) at equilibrium, q_e is the amount of metal ions adsorbed per gram of adsorbent at equilibrium (mg/g adsorbent), b and q_m are the Langmuir constants ascribed to the energy of adsorption and the maximum adsorption capacity, respectively. The coefficients q_m mg/g adsorbent) and b (m/g) can be calculated from a plot of C_e/q_e versus C_e. For our experiments, the sorption data for Cu^{2+} with GO adsorbent were fitted into the linearized Langmuir equation and the obtained results are shown in Table 3 and Figure 9.

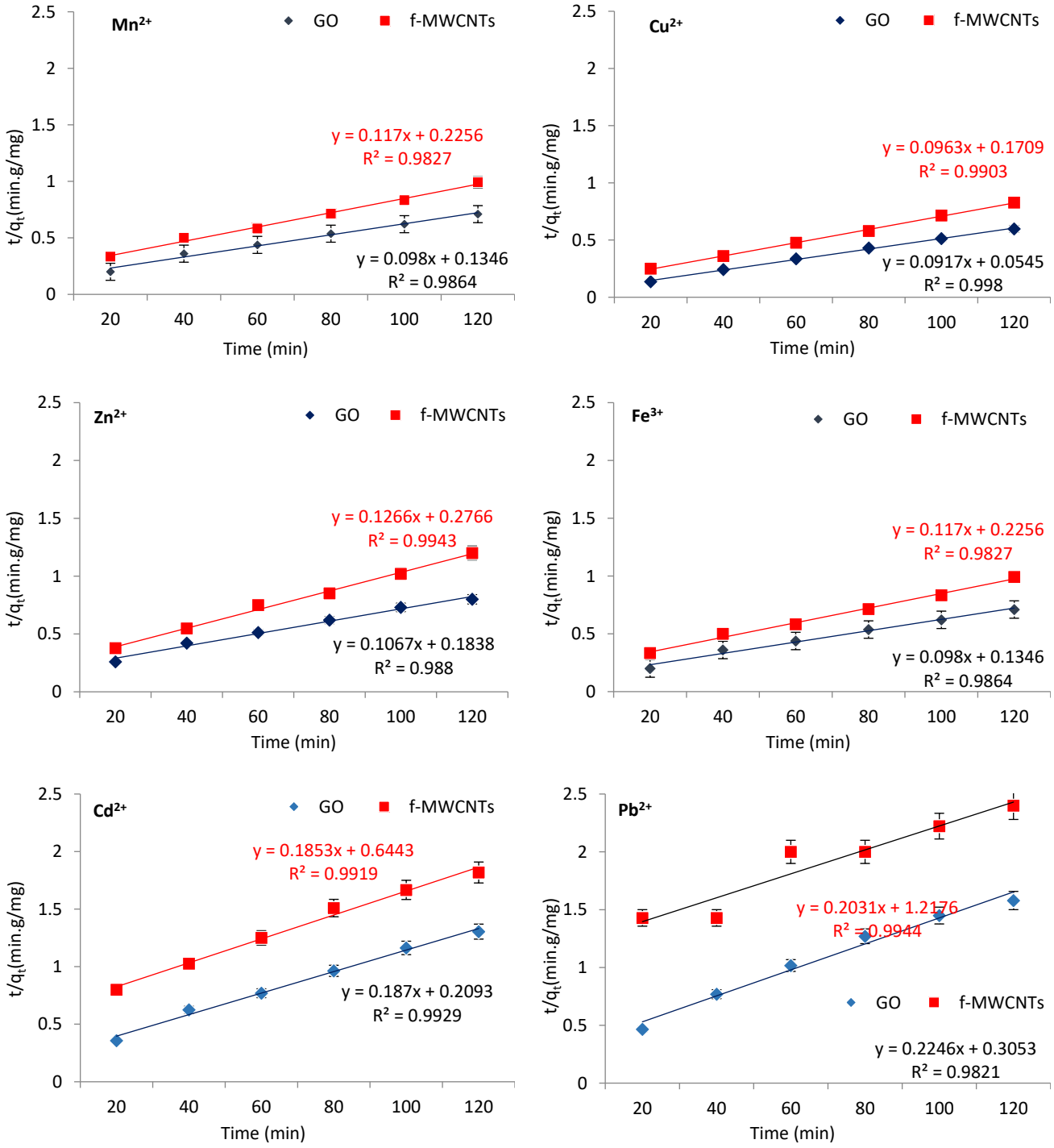

Fig. 8. Pseudo-second-order kinetic plots for ion sorption onto f-MWCNTs and GO.

3.5 . Effect of pH

The pH value plays an important role on the adsorption uptake of different ions with sorbents [31]. The pH of solution severely affects the solubility of the metal ions, the surface charge of the adsorbent and the degree of ionization and speciation of the adsorbates. As seen in Figure 10, as the initial solution pH increased, the adsorption uptake also increased for both adsorbents. The oxidation treatment of f-MWCNTs with concentrated HNO_3/H_2SO_4 led to surface functionalization by the acidic groups, and the pH of the solution affected the surface charge. The adsorption uptake reached the maximum at pH=7 due to the effect of the functional groups formed on the f-MWCNTs surface during oxidation. At pH values below 4, the adsorption uptake was poor because of the competition between M^{2+} ions and H^+ ions in the solution. For the GO, the functional groups on the surface were more

anionic at a higher pH value and this may have made a significant contribution to the metal ion removal by chemsorption. At a pH < pH_{pzc} (pH of point of zero charge), the surface charge of GO was positive due to the protonation reaction as shown in Eq. 4. The positive metal ions were difficult to adsorb on the positively charged surface of GO because of electrostatic repulsion. At a pH > pH_{pzc}, the deprotonation reaction made the surface charge of GO negative [4] (Eq. 5)

$$\_SOH + H^+ \rightarrow \_SOH_2^+ \quad (4)$$

$$\_SOH \rightarrow \_SO^- + H^+ \quad (5)$$

In which, _S and _OH show the nanoadsorbent surface and oxygen-containing functional groups, respectively.

The reaction for hydroxide generation of ions (M^{2+}) can also be summarised as follows (Eq. 6):

$$M^{2+} \leftrightarrow \_M(OH)^+ \leftrightarrow \_M(OH)_2^0 \leftrightarrow \_M(OH)_3^- \quad (6)$$

Metal ions could be jointed with deprotonated surface sites, and the ion sorption on the nanosorbents could be expressed by the reaction summarised below in Eq. 7:
Metal ions could be jointed with deprotonated surface sites, and the ion sorption on the nanosorbents could be expressed by the reaction summarised below in Eq. 7:

$$2\_SO^-_{(s)} + M^{2+}_{(eq)} \rightarrow [(\_SO^-)_2\, M^{2+}]_{(s)} \quad (7)$$

Table 2. Langmuir constants.

Model	Linear Eqs.	Plot	Calculated coefficient
Langmuir	$\frac{C_e}{q_e} = \frac{1}{q_m K_L} + \frac{C_e}{q_f}$	$\frac{C_e}{q_e}$ vs C_e	$K_L = \frac{\text{Slope}}{\text{Intercept}}$ q_m= Slope^{-1}

Table 3. Langmuir constants at three different temperatures for Cu^{2+} onto the GO nanosheets

Temperature/°C	R^2	Eqs	Q_m	b
25	0.998	$Y = 0.0159X + 0.254$	62.89	0.069
30	0.971	$Y = 0.0132X + 0.221$	75.75	0.059
35	0.996	$Y = 0.0120X + 0.224$	83.33	0.054

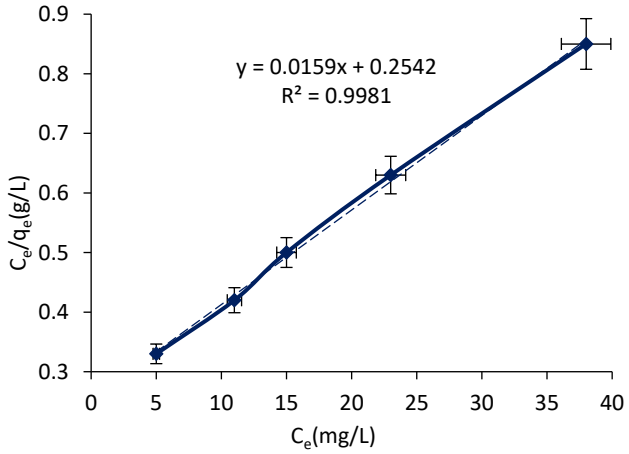

Fig. 9. Linearized Langmuir isotherm for Cu^{2+} sorption in the presence of GO (Contact time= 120min, T=25°C).

3.6. Removal of toxic metal ions from natural AMD wastewater

In order to further study how GO and f-MWCNTs work as adsorbents, AMD wastewater from the Sungun copper mine was tested as a field sample and the results are represented in Figure 11. AMD wastewater was gathered from the low grade sulphur deposit in the Sungun copper mine shown in Figure 12. For the field sample, 1000 ml of the AMD sample including metal ions and 0.1 g of adsorbents were fed into the reactor. The concentrations of Cu^{+2}, Mn^{+2}, Cd^{+2}, Zn^{+2}, Fe^{3+} and Pb^{+2} ions in AMD sample were 228.1, 112.4, 35.9, 91.7, 73.7 and 35.1 mg/L, respectively. Also, the pH of the AMD sample used in this research was 3.7. So, the concentrations of ions in this case study were high and severely polluted the mine environment. The GO showed high total metal ion removal efficiency. The removal efficiency comparison of the Sungun AMD wastewater via GO and f-MWCNTs showed that the GO notably revealed the highest removal efficiency of total ions. The removal efficiency comparison of the Sungun AMD wastewater via GO and f-MWCNTs showed that the GO notably revealed the highest removal efficiency of total ions.

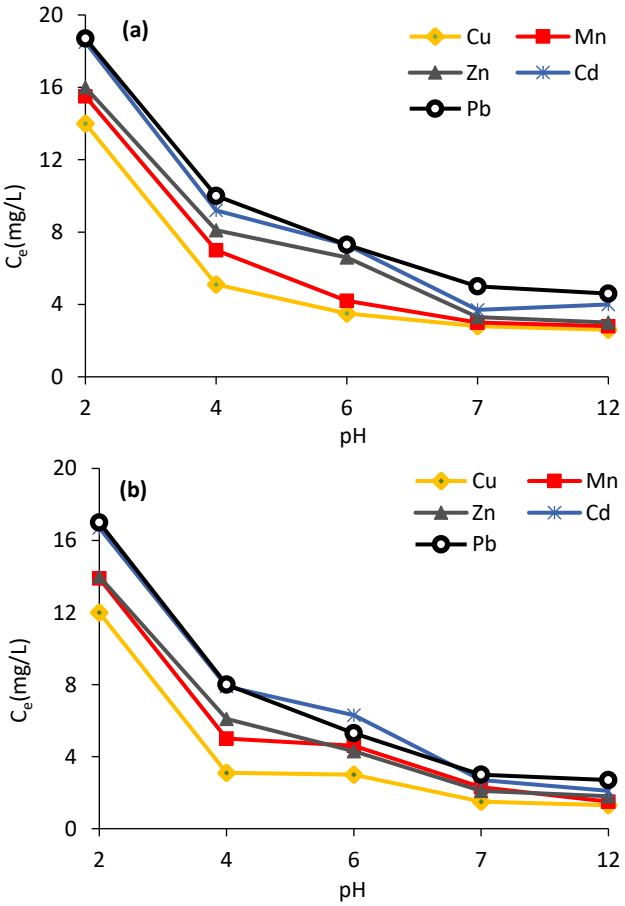

Fig. 10. pH effect on the ion sorption process in the presence of (a) f-MWCNTs and (b) GO. (Contact time=120min, T=25°C).

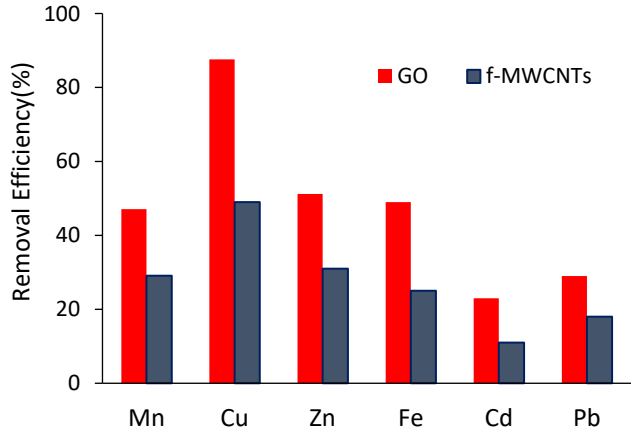

Fig. 11. Removal efficiency of metal ions from AMD wastewater of Sungun copper mine with GO and f-MWCNTs.

Fig. 12. AMD sampling from Sungun Copper Mine.

4. Conclusions

In summary, the GO nanosheets and f-MWCNTs were synthesized and characterized using various techniques. Prepared adsorbents were used for the removal of metal ions from a prepared aqueous solution and actual samples of mine related AMD from the Sungun copper mine. Analysis of the sorption kinetics and isotherms showed that the ion removal obeyed the pseudo-second-order kinetics and Langmuir models, respectively. This study demonstrated the feasibility of both GO and f-MWCNTs for fast adsorption and removal of toxic metal ions in aqueous solutions as well as AMD. The sorbent properties such as fast adsorption kinetics, good solvent stability, high adsorption capacity, excellent reusability, ionic strength, and dissolved organic matter insensitive adsorption capacity strongly affected the removal efficiency.

Acknowledgment

This research in the form of research design "Carbon allotrope for fast adsorption and removal of toxic metal ions: A case study from the Sungun copper mine" has been done with the support of the Islamic Azad University, South Tehran Branch. In addition, the authors are grateful to the anonymous reviewers for their comments on an earlier version of this paper.

References

[1] Kalin, M., Fyson, A., Wheeler, W. N. (2006). The chemistry of conventional and alternative treatment systems for the neutralization of acid mine drainage. *Science of the total environment*, *366*(2), 395-408.

[2] Matlock, M. M., Howerton, B. S., Atwood, D. A. (2002). Chemical precipitation of heavy metals from acid mine drainage. *Water research*, *36*(19), 4757-4764.

[3] Mayer, K. U., Benner, S. G., Blowes, D. W. (2006). Process-based reactive transport modeling of a permeable reactive barrier for the treatment of mine

drainage. *Journal of contaminant hydrology, 85(3*), 195-211.

[4] Motsi, T., Rowson, N. A., Simmons, M. J. H. (2009). Adsorption of heavy metals from acid mine drainage by natural zeolite. *International journal of mineral processing, 92(1)*, 42-48.

[5] Rios, C. A., Williams, C. D., Roberts, C. L. (2008). Removal of heavy metals from acid mine drainage (AMD) using coal fly ash, natural clinker and synthetic zeolites. *Journal of hazardous materials, 156(1),* 23-35.

[6] Sheoran, A. S., Sheoran, V. (2006). Heavy metal removal mechanism of acid mine drainage in wetlands: a critical review. *Minerals engineering, 19(2)*, 105-116.

[7] Johnson, D. B., Hallberg, K. B. (2005). Acid mine drainage remediation options: a review. *Science of the total environment, 338(1)*, 3-14.

[8] Hasanzadeh, R., Moghadam, P. N., Bahri-Laleh, N., Sillanpää, M. (2017). Effective removal of toxic metal ions from aqueous solutions: 2-Bifunctional magnetic nanocomposite base on novel reactive PGMA-MAn copolymer@ Fe_3O_4 nanoparticles. *Journal of colloid and interface science, 490*, 727-746.

[9] Ivanets, A. I., Srivastava, V., Kitikova, N. V., Shashkova, I. L., Sillanpää, M. (2017). Non-apatite Ca-Mg phosphate sorbent for removal of toxic metal ions from aqueous solutions. *Journal of environmental chemical engineering, 5(2)*, 2010-2017.

[10] Mahida, V. P., Patel, M. P. (2014). Synthesis of new superabsorbent poly (NIPAAm/AA/N-allylisatin) nanohydrogel for effective removal of As (V) and Cd (II) toxic metal ions. *Chinese chemical letters, 25(4)*, 601-604

[11] Saravanan, P., Vinod, V. T. P., Sreedhar, B., Sashidhar, R. B. (2012). Gum kondagogu modified magnetic nano-adsorbent: An efficient protocol for removal of various toxic metal ions. *Materials science and engineering: C, 32(3)*, 581-586.

[12] Wei, X., Viadero, R. C. (2007). Synthesis of magnetite nanoparticles with ferric iron recovered from acid mine drainage: Implications for environmental engineering. *Colloids and surfaces A: Physicochemical and engineering aspects, 294(1)*, 280-286.

[13] Mauter, M. S., Elimelech, M. (2008). Environmental applications of carbon-based nanomaterials. *Environmental science and technology, 42(16)*, 5843-5859.

[14] Pradeep, T. (2009). Noble metal nanoparticles for water purification: a critical review. *Thin solid films, 517(24)*, 6441-6478.

[15] Ruparelia, J. P., Duttagupta, S. P., Chatterjee, A. K., Mukherji, S. O. U. M. Y. A. (2008). Potential of carbon nanomaterials for removal of heavy metals from water. *Desalination, 232(1)*, 145-156.

[16] Giraldo, L., Erto, A., Moreno-Piraján, J. C. (2013). Magnetite nanoparticles for removal of heavy metals from aqueous solutions: synthesis and characterization. *Adsorption, 19(2-4)*, 465-474.

[17] Akhbarizadeh, R., Shayestefar, M. R., Darezereshki, E. (2014). Competitive removal of metals from wastewater by maghemite nanoparticles: a comparison between simulated wastewater and AMD. *Mine water and the environment,* 33(1), 89-96.

[18] Klimkova, S., Cernik, M., Lacinova, L., Filip, J., Jancik, D., Zboril, R. (2011). Zero-valent iron nanoparticles in treatment of acid mine water from in situ uranium leaching. *Chemosphere, 82(8)*, 1178-1184.

[19] Dreyer, D. R., Park, S., Bielawski, C. W., Ruoff, R. S. (2010). The chemistry of graphene oxide. *Chemical society reviews, 39(1)*, 228-240.

[20] Zhao, G., Li, J., Ren, X., Chen, C., Wang, X. (2011). Few-layered graphene oxide nanosheets as superior sorbents for heavy metal ion pollution management. *Environmental science and technology, 45(24)*, 10454-10462

[21] Sreeprasad, T. S., Maliyekkal, S. M., Lisha, K. P., Pradeep, T. (2011). *Reduced graphene oxide–metal/metal oxide composites: facile synthesis and application in water purification. Journal of hazardous materials, 186(1)*, 921-931.

[22] Zhao, G., Ren, X., Gao, X., Tan, X., Li, J., Chen, C., Wang, X. (2011). *Removal of Pb (II) ions from aqueous solutions on few-layered graphene oxide nanosheets. Dalton transactions, 40(41)*, 10945-10952.

[23] Yang, S. T., Chang, Y., Wang, H., Liu, G., Chen, S., Wang, Y., Cao, A. (2010). *Folding/aggregation of graphene oxide and its application in Cu^{2+} removal. Journal of colloid and interface science, 351(1)*, 122-127.

[24] Rao, G. P., Lu, C., Su, F. (2007). Sorption of divalent metal ions from aqueous solution by carbon nanotubes: a review. *Separation and purification technology, 58(1)*, 224-231.

[25] Stafiej, A., Pyrzynska, K. (2007). Adsorption of heavy metal ions with carbon nanotubes. *Separation and purification technology, 58(1)*, 49-52.

[26] Agboola, A. E., Pike, R. W., Hertwig, T. A., Lou, H. H. (2007). Conceptual design of carbon nanotube processes. *Clean technologies and environmental policy, 9(4)*, 289-311.

[27] Rahimi, E., Mohaghegh, N. (2016). Removal of toxic metal ions from sungun acid rock drainage using mordenite zeolite, graphene nanosheets, and a novel metal–organic framework. *Mine water and the environment, 35(1)*, 18-28.

[28] Mohaghegh, N., Tasviri, M., Rahimi, E., Gholami, M. R. (2015). Comparative studies on Ag_3PO_4/$BiPO_4$–metal-organic framework–graphene-based nanocomposites for photocatalysis application. *Applied surface science, 351*, 216-224.

[29] Mohaghegh, N., Faraji, M., Gobal, F., Gholami, M. R. (2015). Electrodeposited multi-walled carbon

nanotubes on Ag-loaded TiO_2 nanotubes/Ti plates as a new photocatalyst for dye degradation. *RSC advances, 5(56)*, 44840-44846.

[30] Motsi, T., Rowson, N. A., Simmons, M. J. H. (2009). Adsorption of heavy metals from acid mine drainage by natural zeolite. *International journal of mineral processing, 92(1)*, 42-48.

[31] Wang, F., Pan, Y., Cai, P., Guo, T., Xiao, H. (2017). Single and binary adsorption of heavy metal ions from aqueous solutions using sugarcane cellulose-based adsorbent. *Bioresource technology. 241*, 482-490.